BioOne COMPLETE

Facilitated NaCl Uptake in the Highly Developed Bundle of the Nephron in Japanese Red Stingray Hemitrygon akajei Revealed by Comparative Anatomy and Molecular Mapping

Authors: Aburatani, Naotaka, Takagi, Wataru, Wong, Marty Kwok-Sing, Kadota, Mitsutaka, Kuraku, Shigehiro, et al.

Facilitated NaCl Uptake in the Highly Developed Bundle of the Nephron in Japanese Red Stingray *Hemitrygon akajei* Revealed by Comparative Anatomy and Molecular Mapping

Naotaka Aburatani[1]*, Wataru Takagi[1]*, Marty Kwok-Sing Wong[1], Mitsutaka Kadota[2], Shigehiro Kuraku[2], Kotaro Tokunaga[3], Kazuya Kofuji[3], Kazuhiro Saito[4], Waichiro Godo[4], Tatsuya Sakamoto[4], and Susumu Hyodo[1]

[1]*Laboratory of Physiology, Atmosphere and Ocean Research Institute, The University of Tokyo, Kashiwa 277-8564, Japan*
[2]*Laboratory for Phyloinformatics, RIKEN Center for Biosystems Dynamics, Kobe 650-0047, Japan*
[3]*Ibaraki Prefectural Oarai Aquarium, Oarai 311-1301, Japan*
[4]*Ushimado Marine Institute, Faculty of Science,Okayama University, Ushimado 701-4303, Japan*

Batoidea (rays and skates) is a monophyletic subgroup of elasmobranchs that diverged from the common ancestor with Selachii (sharks) about 270 Mya. A larger number of batoids can adapt to low-salinity environments, in contrast to sharks, which are mostly stenohaline marine species. Among osmoregulatory organs of elasmobranchs, the kidney is known to be dedicated to urea retention in ureosmotic cartilaginous fishes. However, we know little regarding urea reabsorbing mechanisms in the kidney of batoids. Here, we performed physiological and histological investigations on the nephrons in the red stingray (*Hemitrygon akajei*) and two shark species. We found that the urine/plasma ratios of salt and urea concentrations in the stingray are significantly lower than those in cloudy catshark (*Scyliorhinus torazame*) under natural seawater, indicating that the kidney of stingray more strongly reabsorbs these osmolytes. By comparing the three-dimensional images of nephrons between stingray and banded houndshark (*Triakis scyllium*), we showed that the tubular bundle of stingray has a more compact configuration. In the compact tubular bundle of stingray kidney, the distal diluting tubule was highly developed and frequently coiled around the proximal and collecting tubules. Furthermore, co-expression of NKAα1 (Na⁺/K⁺-ATPase) and NKCC2 (Na⁺-K⁺-2Cl⁻ cotransporter 2) mRNAs was prominent in the coiled diluting segment. These findings imply that NaCl reabsorption is greatly facilitated in the stingray kidney, resulting in a higher reabsorption rate of urea. Lowering the loss of osmolytes in the glomerular filtrate is likely favorable to the adaptability of batoids to a wide range of environmental salinity.

Key words: Batoidea, urine, osmoregulation, nephron, membrane transporter, cartilaginous fishes, elasmobranch

INTRODUCTION

Marine cartilaginous fishes (sharks, skates, rays, and chimaeras) are ureosmotic animals and they accumulate high concentrations of urea (300–450 mM) in their body fluids to maintain an osmolality slightly higher than the surrounding seawater (SW), protecting them against dehydration (Smith, 1929, 1936). This unique adaptive strategy and the osmoregulatory organs involved have been well described in previous studies (Pärt et al., 1998; Fines et al.,

2001; Kajimura et al., 2006; Takagi et al., 2012; Hyodo et al., 2014). Among the osmoregulatory organs, the kidney possesses an elaborate urea-reabsorption system to reduce the loss of urea into the environment (see Hyodo et al., 2014). Previous studies demonstrated that elasmobranchs can reabsorb over 90% of the urea from the glomerular filtrate (Smith, 1936; Kempton, 1953); renal excretion thus accounts for only 4–20% of total urea loss from the body (Goldstein and Forster, 1971; Payan et al., 1973).

In order to retain urea, a unique nephron architecture was evolved in the kidney of marine cartilaginous fishes, which have some of the most complicated nephron architectures among vertebrates (Lacy et al., 1985; Lacy and Reale, 1985b; Hentschel, 1987; Hentschel et al., 1993). Each nephron begins from a renal corpuscle and then forms four loops

that pass alternately through two anatomically distinct regions, a bundle zone and a sinus zone. In the bundle zone, five segments of a single nephron (that is, the descending and ascending segments of the first and third loops and the descending collecting tubule) are wrapped by a peritubular sheath to form a sac-like bundle structure (Lacy and Reale, 1986). Together with the similarly described nephron morphology in holocephalan elephant fish (*Callorhinchus milii*; Kakumura et al., 2015), it has been generally accepted that this basic structure of the nephron is shared among cartilaginous fishes.

Beyond these descriptions of the morphological structure, the recent increase in molecular data on membrane transporters has elucidated the urea-reabsorbing mechanism in this unique nephron type (Hyodo et al., 2014). Facilitative membrane urea transporter (UT) locates in the collecting tubule, suggesting that this segment is the major urea reabsorption site (Hyodo et al., 2004; Yamaguchi et al., 2009). A steep concentration gradient of urea is likely generated by the third loop of the nephron, where basolateral Na^+/K^+-ATPase (NKAα1) and apical Na^+-K^+-$2Cl^-$ cotransporter 2 (NKCC2, Slc12a1) are co-expressed (Kakumura et al., 2015; Imaseki et al., 2019). Active uptake of sodium and chloride in this segment likely creates a low urea environment inside the bundle. Based on these findings, our group proposed the current model for urea reabsorption in the elaborate nephron (see Discussion and Hyodo et al., 2014).

Modern Chondrichthyes comprises three groups: Holocephali (chimaeras), Selachii (sharks), and Batoidea (skates and rays). Since almost all the species belonging to these clades are ureosmotic animals, it has generally been thought that they inherited an identical renal urea retention mechanism from the last common ancestor. Meanwhile, previous studies reported lower sodium concentrations (180 $\pm$ 16 mM) in the urine of little skate (*Leucoraja erinacea*) (Stolte et al., 1977) compared with those of sharks [249, 283, and 281 mM in the whitespotted bambooshark (*Chiloscyllium plagiosum*), bull shark (*Carcharhinus leucas*) and spiny dogfish (*Squalus acanthias*), respectively] (Thurau et al., 1969; Wong and Chan, 1977; Imaseki et al., 2019), suggesting that the mechanism for urine production in batoids could be different from that in sharks and chimaeras. This notion is supported by the fact that a larger number of batoids can adapt to low-salinity environments, in contrast to sharks, which are mostly stenohaline marine species. In this study, we aimed to compare nephron structure and function between Japanese red stingray (*Hemitrygon akajei*) and Japanese banded houndshark (*Triakis scyllium*) to gain insights on the diversity in the urea-reabsorption mechanisms among cartilaginous fishes.

MATERIALS AND METHODS

Animals

Female red stingrays, *Hemitrygon akajei* (Müller & Henle, 1841) [n = 6, average disc width = 58 $\pm$ 3.2 cm, average body weight (BW) = 7.8 $\pm$ 1.2 kg] were caught in February 2020 in a bay at Ushimado and transported to Ushimado Marine Institute, Okayama University for plasma and urine collection. They were kept in holding tanks filled with running natural SW (34‰) under natural conditions, and were fed with shrimp at least three times a week. For tissue sampling, three more stingrays [average disc width = 40 $\pm$ 6.2 cm, average BW = 2.8 $\pm$ 1.2 kg] were caught in January and May

2018 in the same location and transported to the Atmosphere and Ocean Research Institute (AORI), The University of Tokyo: two females for RNAseq and one male for three-dimensional reconstruction. They were kept in a 500 L holding tank at 20°C under a constant photoperiod (12 L:12 D) for 3 weeks without feeding.

A female Japanese banded houndshark, *Triakis scyllium* (Müller & Henle, 1839) [fork length (FL) = 66.6 cm, BW = 2.3 kg], was collected in Koajiro Bay, near the Misaki Marine Biological Station of The University of Tokyo. It was transported to AORI and kept in a 2,000 L holding tank at 21°C under a constant photoperiod (12 L:12 D). Female cloudy catsharks, *Scyliorhinus torazame* (Tanaka, 1908) [n = 6, average FL = 39.7 $\pm$ 0.7 cm, average BW = 398.0 $\pm$ 21.2 g] were transported from the Ibaraki Prefectural Oarai Aquarium to AORI and were kept in a 1000 L or 3000 L holding tank filled with natural SW (37‰) at 16°C under a constant photoperiod (12 L:12 D). Catshark rather than houndshark was used for urine collection because of the smaller body size and less active character. The houndshark and catsharks were fed with diced squid and sardine twice a week. All animal experiments were conducted according to the Guidelines for Care and Use of Animals approved by the committees of The University of Tokyo and Okayama University.

Sampling of tissue, plasma, and urine

For tissue sampling, the fish were anesthetized with 0.02% (w/v) ethyl 3-aminobenzoate methanesulfonate (Sigma-Aldrich, MO, USA) buffered with an equal amount of sodium bicarbonate (Sigma-Aldrich). After the whole (left and right halves) kidney was dissected out, one half was immediately frozen in liquid nitrogen and kept at −80°C until RNA extraction, while the other half was fixed in Bouin's solution without acetic acid (saturated picric acid: formalin = 3:1) for 2 days and then stored in 70% ethanol at 4°C until use.

For plasma and urine sampling, the stingrays and catsharks were anesthetized as described above. Blood samples were collected from the dorsal vasculature by a syringe with 0.1% (w/v) EDTA-2K as an anticoagulant and were centrifuged at 10,000 $\times$ g at 4°C for 10 min to obtain the plasma. Only females were used for collecting urine, since Kempton (1953) pointed out the possibility of contaminations of urine by seminal fluid in male individuals. Sexually mature stingray and catshark possess a recognizable opening of the urinary tract, which protrudes to the outside. By using a polyethylene cannula (SP-45, Natsume Seisakusyo, Tokyo, Japan) attached to a collecting device (Supplementary Figure S1), samples of excreted urine were collected from free-swimming animals without contamination by SW or any other body fluids. Sodium and chloride ion concentrations, and osmolality were measured with an atomic absorption spectrophotometer (Z5300, Hitachi, Tokyo, Japan), a digital chloridometer (C-50AP, Jokoh, Japan), and a vapor pressure osmometer (5520/5600, Wescor, UT, USA), respectively. Urea concentration was measured by the colorimetric assay according to Rahmatullah and Boyde (1980).

Library preparation for RNA-seq and sequencing

Total RNA extracted from the frozen kidney of stingray with ISOGEN (Nippon Gene, Toyama, Japan) was treated with DNase I (Thermo Fisher Scientific, MA, USA) to digest genomic DNA and was purified using the Zymo RNA Clean & Concentrator column (Zymo Research, CA, USA). Concentration and length distribution of the RNA was checked with the Qubit RNA HS Assay Kit on a Qubit 2.0 Fluorometer (Thermo Fisher Scientific) and the RNA 6000 Nano Kit on a 2100 Bioanalyzer (Agilent Technologies, CA, USA). Sequencing libraries were prepared using 1 μg of the DNase I-treated total RNA with the TruSeq Stranded mRNA Sample Prep Kit (Illumina, CA, USA) and the TruSeq single-index adaptor (Illumina). RNA fragmentation was performed at 94°C for a shortened duration of 4 minutes, compared to the standard condition (94°C for 8 minutes) to generate libraries with longer insert size distribution (Hara et al., 2015). The optimal numbers of PCR cycles for the

libraries were pre-determined to be 7 cycles using the KAPA Real-Time Library Amplification Kit (Roche Applied Science, Mannheim, Germany) as described previously (Kadota et al., 2017). Libraries were sequenced with the Rapid Run mode of HiSeq1500 (Illumina) using the HiSeq PE Rapid Cluster Kit ver2 (Illumina) and the HiSeq Rapid SBS Kit v2-HS (Illumina), and paired-end reads of 127 bases were produced. Base-calling was performed with RTA ver1.18.64, and the fastq files were generated with bcl2fastq ver1.8.4 (Illumina). The raw sequenced reads were deposited in the DNA Data Bank of Japan (DDBJ) under the accession number **DRA009804**.

cDNA cloning and RNA probe synthesis

Total RNA was extracted from the frozen kidney of stingray with ISOGEN (Nippon Gene). Two micrograms of total RNA were treated with DNase using a TURBO DNA-free kit (Thermo Fisher Scientific) and reverse-transcribed to first-strand cDNA using a high-capacity cDNA reverse transcription kit (Thermo Fisher Scientific), according to the manufacturer's protocols. Primer sets were designed to amplify cDNAs encoding NKAα1 (837 bp; GenBank accession no. **LC530055**), NKCC2 (768 bp; **LC530056**), and UT (1004 bp; **LC530057**) based on the contig sequence data from the in-house transcriptome database as mentioned above (Supplementary Table S1). PCR was performed with KAPA Taq Extra (Kapa Biosystems, MA, USA) by using the kidney cDNA as template. The amplified products were electrophoresed on agarose gels, excised and ligated into pGEM-T Easy Vector (Promega, WI, USA). The nucleotide sequence was confirmed by an automated DNA sequencer (ABI PRISM 3100, Applied Biosystems, CA, USA). For digoxigenin (DIG)-labeled RNA probe synthesis, a DNA fragment was amplified again from the sequenced plasmid by PCR with Primestar GXL (Takara Bio, Shiga, Japan) using the M13 Forward and Reverse primers and subsequently purified with Wizard SV Gel and PCR Clean-Up System (Promega). Antisense and sense RNA probes were then synthesized from the purified template using a DIG RNA labeling kit (Roche Applied Science), following the manufacturer's protocols.

In situ hybridization and morphological observation

The fixed kidney was embedded in Paraplast (McCormick Scientific, IL, USA). Serial sections were cut at 7 µm thickness and mounted onto MAS-GP-coated slides (Matsunami Glass, Osaka, Japan). Hybridization and washing were conducted according to a protocol previously described by Takabe et al. (2012). Stained sections were counterstained with Kernechtrot Stain Solution (MUTO PURE CHEMICALS, Tokyo, Japan). For morphological observations, kidney sections were stained with periodic acid–Schiff (PAS; McManus, 1946). Briefly, deparaffinized sections were oxidized in 0.5% periodic acid solution (Wako) for 5 min. After washing in tap water and distilled water, sections were placed in Schiff's reagent (Wako) for 15 min, and then rinsed with wash solution (10% sulfurous acid:1N hydrochloric acid:distilled water = 24 mL:20 mL:400 mL) three times. Sections were then counterstained with Mayer's hematoxylin (Wako). Stained sections were mounted with Permount (Thermo Fisher Scientific). Micrographs were obtained using a virtual slide system (BZ-X800 and accompanying software, Keyence, Osaka, Japan) and a digital camera (DXM1200; Nikon, Tokyo, Japan).

Three-dimensional reconstruction of stained serial sections

To reconstruct the nephrons of stingray, serial paraffin sections (480 sections in total) were divided into four series (A to D). As illustrated in Supplementary Figure S2, the first two sections were mounted on a slide A1, and the next two sections were mounted on a slide B1. Finally, six sections were mounted on a slide, and 80 slides (20

slides for each of series A, B, C and D) were prepared in total. Slides of the series A were treated with PAS-hematoxylin staining, and slides of the series B, C and D were stained with in situ hybridization of NKAα1, NKCC2 and UT mRNAs, respectively. This enabled us to conduct reconstruction of nephron structure and mapping of transporter expressions simultaneously. For the houndshark nephron, serial sections (300 sections in total) were mounted onto one series of slides and stained by PAS-hematoxylin only, since the mapping of NKAα1, NKCC2 and UT was previously described (Hyodo et al., 2004; Imaseki et al., 2019). To obtain the three-dimensional (3D) images of a single nephron, each segment was highlighted by different colors using GIMP 2.8. The highlighted regions were then aligned and stacked by using StackReg and TurboReg plugins of ImageJ (Abràmoff et al., 2004). Finally, 3D images of the stacked sections were generated using the 3D Viewer plugin of ImageJ.
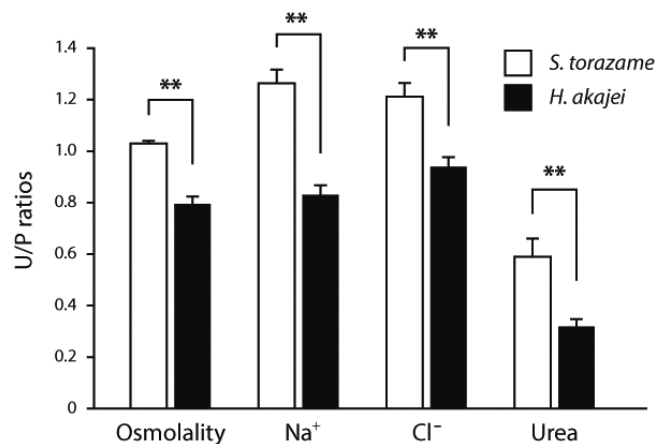
Statistical analysis

Values are presented as means ± s.e.m. Plasma parameters of stingray were largely different from those of catshark, most likely due to the difference in the baselines of the surrounding SW. Therefore, in this study, the original values of each parameter were not compared statistically. Comparisons of urine/plasma (U/P) ratio of each parameter between the stingray and catshark were performed with the Mann-Whitney U test. All P values were two-tailed, and $P < 0.05$ was considered statistically significant. Statistical analysis was performed by using KyPlot 6.0 software (Kyenslab, Tokyo, Japan).

RESULTS

Urea and ionic composition of plasma and urine in two elasmobranchs

Table 1 shows the concentrations of Na$^+$ and Cl$^-$, and

Fig. 1. The urine/plasma (U/P) ratio of each parameter shown in Table 1. Statistical analysis was performed by using the Mann-Whitney U test. Statistically significant differences between stingray and catshark are shown with asterisks (**$P < 0.01$).

Table 1. Plasma and urine parameters of stingray and catshark ($n = 6$ for each).

		Osmolality (mOsm/kg)	Na$^+$ (mM)	Cl$^-$ (mM)	Urea (mM)
SW (Ushimado)		946.5	488.5	456.4	0.0
H. akajei	plasma	944.5 ± 10.0	337.2 ± 3.8	279.3 ± 7.4	273.1 ± 4.3
	urine	749.6 ± 26.7	278.2 ± 16.3	259.7 ± 5.0	86.4 ± 8.5
SW (AORI)		1063.5	608.1	578.5	0.0
S. torazame	plasma	976.9 ± 1.6	309.7 ± 4.6	234.6 ± 1.1	340.5 ± 8.6
	urine	1002.2 ± 11.1	390.3 ± 18.1	283.9 ± 11.3	216.2 ± 23.4

Note. Values are presented as means ± s.e.m.

urea, and osmolality in the plasma and urine of stingray and catshark. The salinity of the holding water in the experiment with stingray was lower (osmolality, 946.5 mOsm/kg; Na$^+$, 488.5 mM; Cl$^-$, 456.4 mM) than that with catshark (osmolality, 1063.5 mOsm/kg; Na$^+$, 608.1 mM; Cl$^-$, 578.5 mM) as the sources of natural SW were different. Likewise, the plasma sodium, chloride and urea concentrations and osmolality were lower in stingray (Table 1). Because of this intrinsic difference, we compared the urine/plasma (U/P) ratio of each parameter between the stingray and catshark (Fig. 1). The U/P ratios of all the parameters were significantly lower in the stingray (osmolality, 0.79; Na$^+$, 0.82; Cl$^-$, 0.94; urea, 0.32) than in the catshark (osmolality, 1.03; Na$^+$, 1.26; Cl$^-$,

1.21; urea, 0.60).

Histological observations of the stingray and banded houndshark nephrons

The stingray and houndshark kidneys were composed of multiple lobules, and each lobule was further divided into the bundle and sinus zones, where a line of renal corpuscle was found at the boundary between the two zones (Fig. 2A, B). In the bundle zone of houndshark kidney, we frequently observed cross-sectional views of a typical five-tubular bundle, which is composed of the descending and ascending segments of the first and third loops, and the descending collecting tubule wrapped together by a peritubular sheath
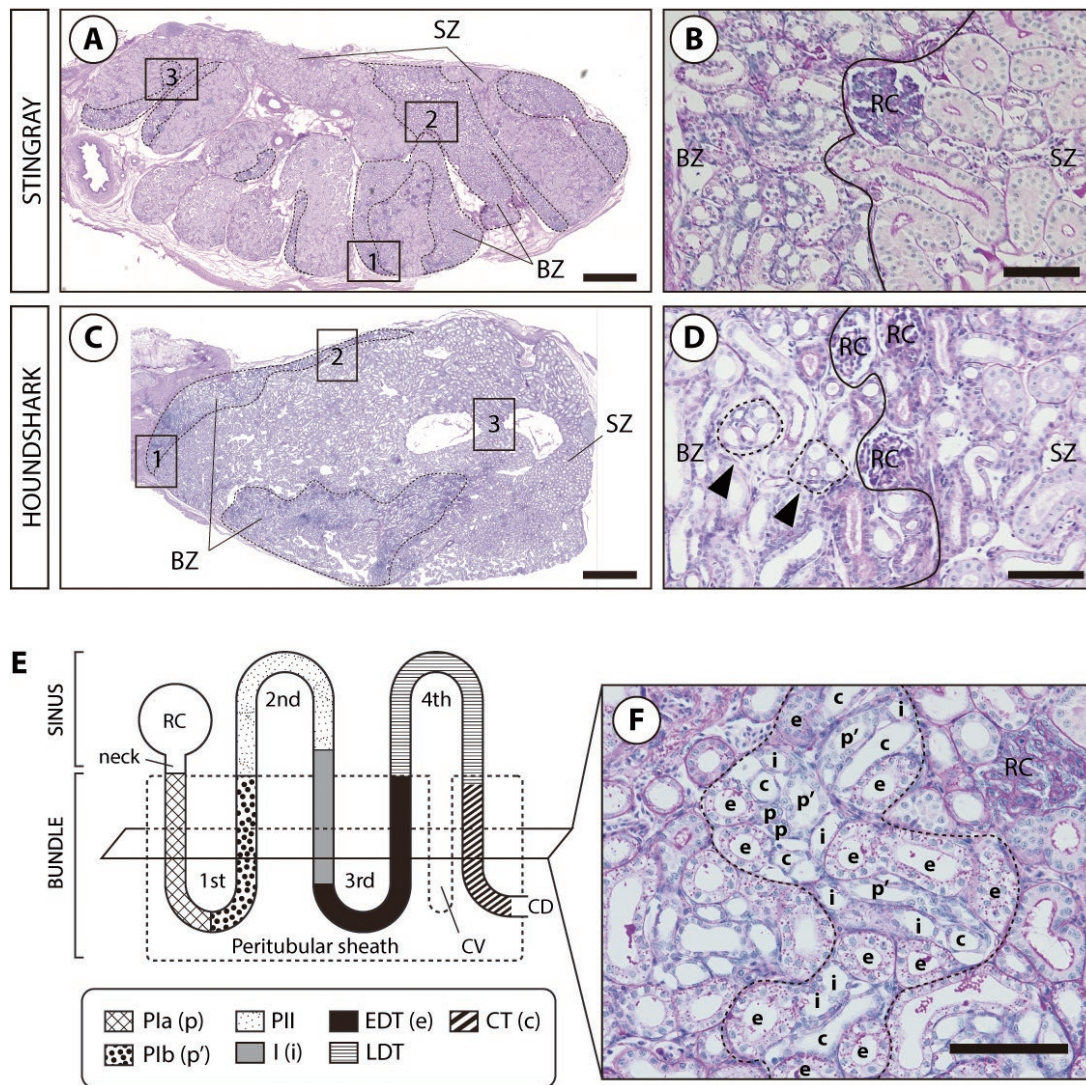
Fig. 2. Stingray and houndshark kidneys. **(A, C)** Low magnification cross-sectional overviews of the halves of the stingray and houndshark kidney, stained with PAS-hematoxylin. The areas surrounded by broken lines represent the bundle zones. Numbered boxes represent the nephrons examined in this study. The 3D images of corresponding nephrons are shown in Fig. 3. BZ, bundle zone; SZ, sinus zone. **(B, D)** Magnified views of the boundary between the BZ and SZ in each animal. Lines represent the boundaries. The tubular bundles containing the five renal tubules of the nephron (circled with broken lines and indicated by black arrowheads) are rarely found in the stingray **(B)** but frequently found in the houndshark **(D)**. RC, renal corpuscle. **(E)** Schematic drawing of the segmentation of the stingray nephron. CV, central vessel; CD, collecting duct. PIa (p), descending proximal I (PI); PIb (p'), ascending PI; PII, proximal II; I (i), intermediate; EDT (e), early distal; LDT, late distal; CT(c), collecting. **(F)** Six types of the renal tubules identified in a single bundle of the stingray nephron (neck segment is not shown). Bars, 1 mm **(A, C)**; 100 μm **(B, D, F)**.

(Fig. 2D). In contrast, such an apparent bundle unit was rarely observed in the stingray kidney (Fig. 2B), suggesting that the composition of the tubular bundle is somewhat different in stingray (see 3D nephron result below).

We selected three representative nephrons from the kidneys of stingray and houndshark (Fig. 2A, C), for examination of the histological and morphological characteristics of nephron segments. Based on the histological criteria in PAS-hematoxylin stained serial sections (Kakumura et al., 2015), seven major segments were identified in stingray: 1) neck; 2) proximal I (PI); 3) proximal II (PII); 4) intermediate; 5) early distal (EDT); 6) late distal (LDT); and 7) collecting (CT) (Fig. 2E, F). These classifications were later confirmed by the 3D reconstructed images. The proximal segments (PI and PII) were characterized by apical brush-border membrane and were distributed in the bundle and sinus zones, respectively (Fig. 2E, F). The PI was further divided into ascending PIa and descending PIb, composed of larger cells. The EDT possessed large columnar cells with apical membrane that was modestly PAS-positive (Fig. 2F). The intermediate segment crossing the bundle and sinus zones was a junctional tubule between the PII and EDT (Fig. 2E, F). In the sinus zone, the LDT was a small tubule composed of thin squamous cells, while the PII had a large diameter tubule with high columnar cells. The collecting tubule was composed of cuboidal cells, and the lumen was PAS-negative (Fig. 2F).

Three-dimensional images of the stingray and houndshark nephrons

By assembling the serial section views, we generated 3D images of the nephrons of stingray and houndshark to investigate the presumed structural differences. As shown in Fig. 3A and B, a distinct difference was observed in the bundle zone; the tubular bundles of the stingray nephron were more compact than those of houndshark. In houndshark, a nephron in the bundle area could be further separated typically into two regions: a straight portion and a convoluted portion, as seen in Fig. 3B-2. The straight portion composed of the five tubular segments started in close association with the renal corpuscle and extended into the bundle zone, while the convoluted region was located at the periphery of the bundle zone and was composed mainly of EDT (orange tubules in Fig. 3B, D). In stingray, all of the bundles examined were dense and compact (Fig. 3A). The straight portion was absent or confined to a short segment near the renal corpuscle. The PI (descending and ascending segments of the first loop) and collecting tubule in the bundle were coiled around by the EDT to form a compact convoluted structure (Fig. 3A, C). All the structural characteristics of tubular bundles were consistent among all the nephrons examined so far in both species (Fig. 3).

Distributions of membrane transporters in nephron segments

In addition to the 3D reconstructions of nephrons, we conducted in situ hybridization to investigate the distribution of three major membrane transporters (NKAα1, NKCC2,
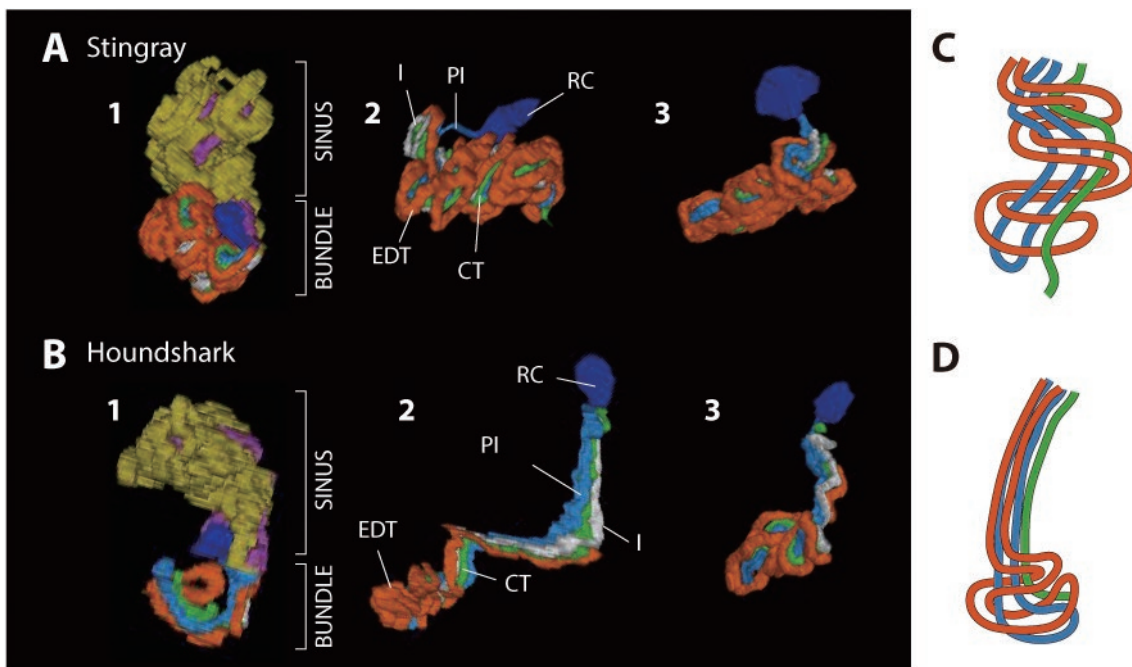
Fig. 3. **(A, B)** Three-dimensional (3D) images reconstructed by using serial sections of the stingray **(A)** and houndshark **(B)** nephrons. Each component of the nephrons colored with dark blue, blue, yellow, white, orange, purple and green represent the renal corpuscle, PI, PII, intermediate, EDT, LDT and CT, respectively. For nephrons of **(A-1)** and **(B-1)**, the images of whole nephron including the tubules both in the bundle zone and sinus zone are shown. For nephrons of **(A-2)**, **(A-3)**, **(B-2)**, and **(B-3)**, only the images of bundle were represented by omitting the tubules in the sinus zone. **(C, D)** Schematic drawings of the tubular configuration in the bundle zone of representative nephron in the stingray and houndshark, respectively. See Fig. 2 for the abbreviations.
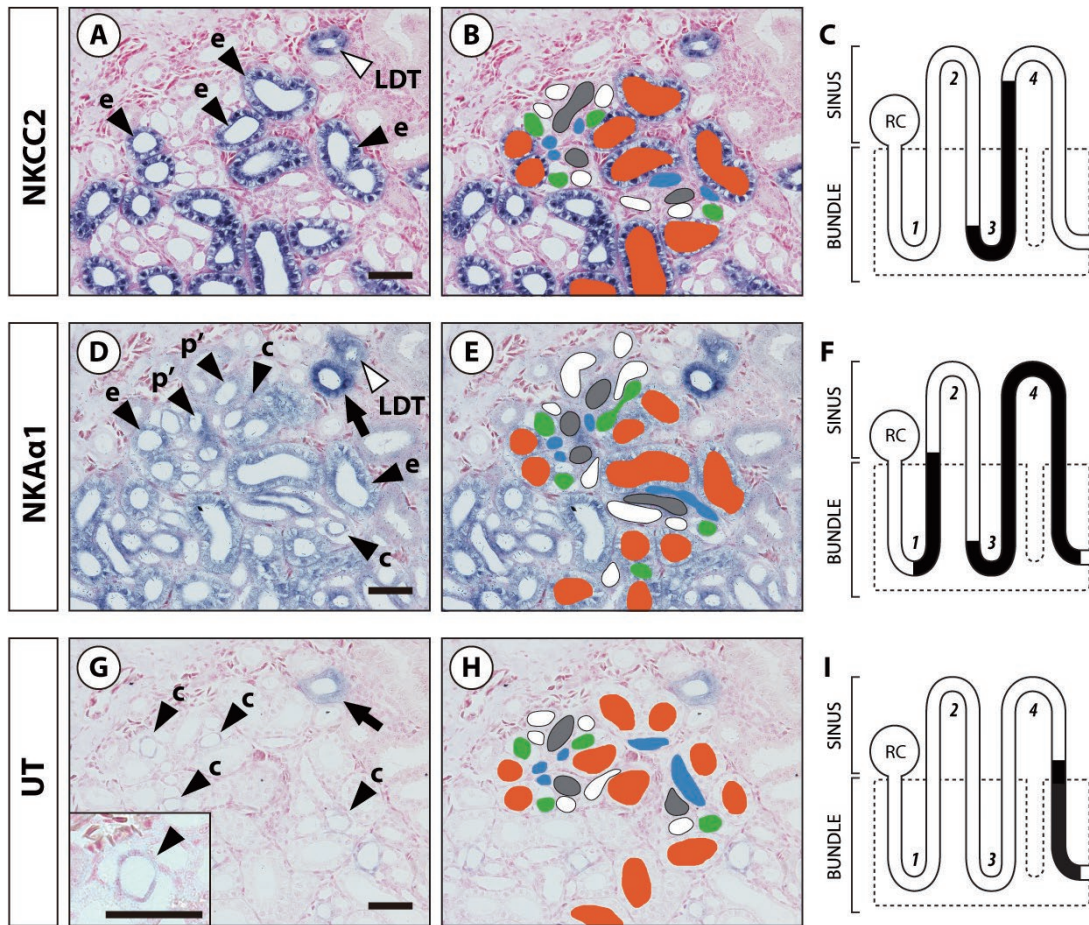
Fig. 4. **(A, D, G)** Localization of the stingray NKCC2, NKAα1, and UT mRNAs in the bundle zone detected by in situ hybridization. **(B, E, H)** With the serial sections that were used for 3D reconstruction, the tubules that originated from a single renal corpuscle were identified. The tubules colored blue, gray, white, orange, and green represent the PIa, PIb (p'), intermediate (i), EDT (e) and CT (c), respectively, as shown in the left panels **(A, D, G)**. Each micrograph is identical to the left panels **(A, D, G)**. **(C, F, I)** Schematic illustrations of the distributions for NKCC2, NKAα1, and UT mRNAs. **(A)** The intense signals of NKCC2 mRNA were found in the EDT of the bundle (e, indicated by closed arrowheads) and also found in the ascending portion of the LDT (open arrowhead). **(D)** In the bundle zone, the NKAα1 signals were widely found in the PIb (p'), EDT (e), and CT (c) (closed arrowheads). In the sinus zone, ascending portion of the LDT (open arrowheads) and the transitional portion (arrow) where the LDT enters the bundle and becomes CT express NKAα1. **(G)** The UT expression was found in the CT of the bundle (closed arrowheads) and the transitional portion of the LDT (arrow). The inset of **(G)** is high magnification showing the UT signal in the CT (c). See Figs 2 and 3 for the abbreviations. Bars, 50 µm.

and UT), which have been considered to be important for urea reabsorption in the tubular bundle. The localization of these transporters was already established in houndshark, as well as in elephant fish and bull shark (Hyodo et al., 2004; Kakumura et al., 2015; Imaseki et al., 2019). In the houndshark nephron, NKAα1 and NKCC2 mRNAs were co-expressed in the EDT and LDT, while UT mRNA was localized in the collecting tubule (Imaseki et al., 2019). In the stingray nephron, intense NKCC2 mRNA signals were found in the EDT and the first-half of the LDT (Fig. 4A–C). The expression of NKCC2 mRNA was mostly co-localized with the signals of NKAα1 mRNA (Fig. 4A–F). UT mRNA expression was found in the collecting tubule and the preceding transitional region where the LDT entered the bundle and became the collecting tubule (Fig. 4G–I). In addition to its location in the EDT and LDT, NKAα1 mRNA expression was also observed in the collecting tubule and the ascending segment of the first loop (PIb) (Fig. 4D–F).

DISCUSSION

For cartilaginous fishes conducting a urea-based osmoregulation, urea retention is required to maintain a high concentration of urea in the body fluid against the steep concentration gradient between body fluid and SW. In the present study, we confirmed that urea concentration in urine was much lower than that in plasma in both stingray and catshark. However, we also found that U/P ratios of sodium, chloride, and urea concentrations were significantly lower in stingray than those in catshark. The results from our stingray measurements are consistent with previous findings in little skate (Payan et al., 1973; Stolte et al., 1977). On the other hand, the urinary sodium, chloride, and urea concentrations observed in cloudy catshark coincided well with the results for other shark species (Wong and Chan, 1977; Imaseki et al., 2019), implying that the low U/P ratios of sodium, chloride, and urea concentrations are common phenomena in

batoids.

By reconstructing the 3D images of nephrons, we found distinct structural differences in the tubular bundles, which may contribute to a higher capacity for sodium and chloride uptake and for urea reabsorption in the stingray. In both the stingray and houndshark, renal lobules were separated into two morphologically distinguishable regions, the bundle and sinus zones, as previously reported for other cartilaginous fish species (Lacy and Reale, 1985a; Hentschel, 1987; Kakumura et al., 2015). Each nephron makes four loops and goes back and forth between two zones, but a distinct difference was found in the bundle zone. The bundle of houndshark was composed of straight and convoluted portions, a feature that was consistent with those found in bull shark and elephant fish (Kakumura et al., 2015; Imaseki et al., 2019). The existence of a straight portion was also shown in the kidney of small-spotted catshark (*S. canicula*), a close relative of cloudy catshark (Hentschel, 1998). In stingray, the architecture of the bundle was dense and compact, and the first loop and the collecting tubule were coiled around by the EDT, indicating that the EDT is highly developed. Hentschel (1998) described the diversity of nephron morphology among elasmobranchs and pointed out that the bundle of the skate nephron was more complex in its structure than the bundle of the small-spotted catshark (*S. canicula*). The morphological description of the skate nephron resembles those of stingray in the present study, indicating that the highly developed EDT is common in batoids.

We also investigated the distribution of mRNAs for NKAα1, NKCC2 and UT, which are major pump and transporter proteins contributing to reabsorption of NaCl and urea in other cartilaginous fishes (Hyodo et al., 2014), in the stingray nephron to compare with those in the houndshark nephron (Imaseki et al., 2019). The molecular mapping approach provides a powerful tool for understanding physiological processes that take place in the highly elaborate kidney (Hyodo et al., 2014; Imaseki et al., 2019). Similar to the distribution in the houndshark kidney, co-expression of NKAα1 and NKCC2 mRNAs was found in the EDT in the tubular bundle, while expression of UT mRNA was predominantly detected in the collecting tubule and the preceding end portion of the LDT. Based on our previously proposed model for urea reabsorption (Hyodo et al., 2014), the first step is active reabsorption of NaCl via the activities of NKAα1 and NKCC2 in the EDT. The resulting increase in osmolality induces reabsorption of water, which creates a low urea micro-environment in the tubular bundle. Urea is then reabsorbed from the collecting tubule via UT using the concentration gradient of urea as a driving force. This model is supported by the finding of a higher sodium and a lower urea concentration in the bundle zone compared to the sinus zone, without differences in osmolality (Hentschel et al., 1986). For the batoids that possess the highly developed EDT in a compact tubular bundle, it is conceivable that reabsorption of NaCl caused by the actions of NKAα1 and NKCC2 is greater than that in sharks, which in turn enhances the overall reabsorption of NaCl and urea. Our molecular histological data corresponded well with the observed low U/P ratios of sodium, chloride and urea in the stingray.

In addition to the EDT, NKAα1 mRNA expression was also detected in the PIb segment and collecting tubule, sug-

gesting that basolateral NKAα1 also functions to generate a driving force for transport of particular solutes in these segments in the tubular bundle. The Na^+-D-glucose cotransporters (SGLTs) are possible candidates for an apical sodium transporter coupled with the basolateral NKAα1 in the PIb, since the immunoreactive signals were found in the proximal tubules of spiny dogfish and little skate nephrons (Althoff et al., 2006, 2007). The facilitative UT has been detected in the collecting tubule of all cartilaginous fishes examined thus far (Hyodo et al., 2004; Kakumura et al., 2015; Imaseki et al., 2019), indicating that urea reabsorption is a common function of collecting tubules. Meanwhile, in euryhaline bull shark, apical Na^+-Cl^- cotransporter (NCC, Slc12a3) was co-expressed with basolateral NKAα1 in the LDT and collecting tubule, and the expression of both mRNAs was upregulated following the transfer to a low-salinity environment, implying that the collecting tubule also contributes to NaCl reabsorption in the tubular bundle (Imaseki et al., 2019). Further studies are necessary to identify the apical transporter(s) that are involved in the solute transport in the PIb segment and the collecting tubule of the stingray nephron.

Batoid (rays and skates) is the largest subgroup of modern cartilaginous fishes, with 633 species (Last et al., 2016). Molecular phylogenetic analysis strongly supports the monophyly of batoids, and the group was diverged from the common ancestor shared by Selachii (sharks) (Douady et al., 2003). Since the batoids have evolved independently of shark relatives, apparent morphological, physiological, and molecular divergences are conceivable. Our data showed the distinct urine compositions and nephron structures between the batoids and sharks, opening up new paths for understanding the evolution that ancestral species of elasmobranchs experienced.

The habitat range and acclimation capacity among the extant elasmobranchs may shed light on such evolutionary events. Most sharks are marine species and only a few (bull shark and *Glyphis*) have the ability to acclimate to low salinity environments, including freshwater (FW). On the other hand, many species of batoids are known to inhabit brackish and/or freshwater environments (Ballantyne and Fraser, 2012). These euryhaline species of cartilaginous fishes (except obligate FW species) retain a considerable amount of NaCl and urea in their body fluids even in FW or diluted SW (Forster and Goldstein, 1976; Piermarini and Evans, 1998; Imaseki et al., 2019). Following the transfer of Atlantic stingray from full-strength SW to 50% SW, tubular reabsorption of NaCl and urea was increased 2.5-fold and 3-fold, respectively (Janech et al., 2006). The increased NaCl reabsorption by the batoid-type bundle might be advantageous for expanding batoids' habitat to low salinity environments (e.g., brackish water of estuaries and FW of rivers and lakes). Indeed, a Chinese subpopulation of red stingray inhabits and probably breeds in a FW environment throughout its entire life (Li et al., 2015). Recently, we reported that the expressions of NCC mRNA in euryhaline bull shark drastically increased in the LDT and the collecting tubule when it was transferred from SW to FW, indicating that NaCl reabsorption via NCC is one of the key renal functions of the bull shark in the FW environment (Imaseki et al., 2019). The kidney of red stingray could have evolved special features for

acclimating to a wide range of salinity, and it could be used as a model to study the molecular mechanism of FW acclimation in batoids.

COMPETING INTERESTS

The authors have no competing interests to declare.

AUTHOR CONTRIBUTIONS

NA and WT designed the study. NA, WT, MKW, MK, and SK performed the experiments and collected data. NA, WT, MKW, KT, KK, KS, WG, and TS kept the animals and contributed to sample collection. NA and WT wrote the first draft of the manuscript, and MKW and SH largely contributed to the revision step. All the authors contributed substantial input to the final version of the manuscript.

SUPPLEMENTARY MATERIALS

Supplementary materials for this article are available online. (URL: https://doi.org/10.2108/zs200038)
Supplementary Table S1. Primer sets used for cDNA cloning and in situ hybridization.
Supplementary Figure S1. The urine collecting device that we developed in this study.
Supplementary Figure S2. Serial paraffin sections of stingray kidney were prepared for PAS-hematoxylin staining, in situ hybridization, and eventual 3D reconstruction.

REFERENCES

Abràmoff MD, Magalhães PJ, Ram SJ (2004) Image processing with ImageJ. Biophotonics Int 11(7): 36–43

Althoff T, Hentschel H, Luig J, Schutz H, Kasch M, Kinne RKH (2006) Na$^+$-D-glucose cotransporter in the kidney of Squalus acanthias: molecular identification and intrarenal distribution. Am J Physiol 290(4): R1094–R1104

Althoff T, Hentschel H, Luig J, Schütz H, Kasch M, Kinne RKH (2007) Na$^+$-D-glucose cotransporter in the kidney of *Leucoraja erinacea*: molecular identification and intrarenal distribution. Am J Physiol 292(6): R2391–R2399

Ballantyne JS, Fraser DI (2012) Euryhaline elasmobranchs. In "Fish Physiology Vol. 32" Ed by S McCormick, A Farrell, C Brauner), Academic Press, Waltham, pp 125–198

Boylan JW (1967) Gill permeability in elasmobranchs. In "Sharks, Skates, and Rays" Ed by PW Gilbert, RF Mathewson, DP Rall), Johns Hopkins Press, Baltimore, pp 197–206

Douady CJ, Dosay M, Shivji MS, Stanhope MJ (2003) Molecular phylogenetic evidence refuting the hypothesis of Batoidea (rays and skates) as derived sharks. Mol Phylogenet Evol 26(2): 215–221

Fines GA, Ballantyne JS, Wright PA (2001) Active urea transport and an unusual basolateral membrane composition in the gills of a marine elasmobranch. Am J Physiol 280(1): R16–R24

Forster RP, Goldstein L (1976) Intracellular osmoregulatory role of amino acids and urea in marine elasmobranchs. Am J Physiol 230(4): 925–931

Goldstein L, Forster RP (1971) Osmoregulation and urea metabolism in the little skate *Raja erinacea*. Am J Physiol 220(3): 742–746

Hara Y, Tatsumi K, Yoshida M, Kajikawa E, Kiyonari H, Kuraku S (2015) Optimizing and benchmarking de novo transcriptome sequencing: from library preparation to assembly evaluation. BMC Genomics 16(1): 977

Hentschel H (1987) Renal architecture of the dogfish Scyliorhinus caniculus (Chondrichthyes, Elasmobranchii). Zoomorphology 107(2): 115–125

Hentschel H, Elger M, Schmidt-Nielsen B (1986) Chemical and morphological differences in the kidney zones of the elasmobranch, *Raja erinacea* Mitch. Comp Biochem Physiol A 84(3): 553–557

Hentschel H, Mähler S, Herter P, Elger M (1993) Renal tubule of dogfish, Scyliorhinus caniculus: A comprehensive study of structure with emphasis on intramembrane particles and immunoreactivity for H$^+$-K$^+$-adenosine triphosphatase. Anat Rec 235(4): 511–532

Hentschel H, Storb U, Teckhaus L, Elger M (1998) The central vessel of the renal countercurrent bundles of two marine elasmobranchs—dogfish (Scyliorhinus caniculus) and skate (Raja erinacea) —as revealed by light and electron microscopy with computer-assisted reconstruction. Anat Embryol 198: 73–89

Hyodo S, Katoh F, Kaneko T, Takei Y (2004) A facilitative urea transporter is localized in the renal collecting tubule of the dogfish Triakis scyllia. J Exp Biol 207(2): 347–356

Hyodo S, Kakumura K, Takagi W, Hasegawa K, Yamaguchi Y (2014) Morphological and functional characteristics of the kidney of cartilaginous fishes: with special reference to urea reabsorption. Am J Physiol 307(12): R1381–R1395

Imaseki I, Wakabayashi M, Hara Y, Watanabe T, Takabe S, Kakumura K, et al. (2019) Comprehensive analysis of genes contributing to euryhalinity in the bull shark, Carcharhinus leucas; Na$^+$-Cl$^-$ co-transporter is one of the key renal factors upregulated in acclimation to low-salinity environment. J Exp Biol 222(12): jeb201780

Janech MG, Fitzgibbon WR, Ploth DW, Lacy ER, Miller DH (2006) Effect of low environmental salinity on plasma composition and renal function of the Atlantic stingray, a euryhaline elasmobranch. Am J Physiol 291(4): F770–F780

Kadota M, Hara Y, Tanaka K, Takagi W, Tanegashima C, Nishimura O, et al. (2017) CTCF binding landscape in jawless fish with reference to Hox cluster evolution. Sci Rep 7(1): 1–11

Kajimura M, Walsh PJ, Mommsen TP, Wood CM (2006) The dogfish shark (*Squalus acanthias*) increases both hepatic and extrahepatic ornithine urea cycle enzyme activities for nitrogen conservation after feeding. Physiol Biochem Zool 79: 602–613

Kakumura K, Takabe S, Takagi W, Hasegawa K, Konno N, Bell JD, et al. (2015) Morphological and molecular investigations of the holocephalan elephant fish nephron: the existence of a countercurrent-like configuration and two separate diluting segments in the distal tubule. Cell Tissue Res 362(3): 677–688

Kempton RT (1953) Studies on the elasmobranch kidney. II. Reabsorption of urea by the smooth dogfish, Mustelus canis. Biol Bull 104(1): 45–56

Lacy ER, Reak E, Schlusselberg DS, Smith WK, Woodward DJ (1985) A renal countercurrent system in marine elasmobranch fish: a computer-assisted reconstruction. Science 227(4692): 1351–1354

Lacy ER, Reale E (1985a) The elasmobranch kidney. I. Gross anatomy and general distribution of the nephrons. Anat Embryol 173(1): 23–24

Lacy ER, Reale E (1985b) The elasmobranch kidney. II. Sequence and structure of the nephrons. Anat Embryol 173(2): 163–186

Lacy ER, Reale E (1986) The elasmobranch kidney. III. Fine structure of the peritubular sheath. Anat Embryol 173(3): 299–305

Last P, Naylor G, Séret B, White W, de Carvalho M, Stehmann M (2016) Rays of the World. CSIRO Publishing, Clayton

Li N, Chen X, Sun D, Song N, Lin Q, Gao T (2015) Phylogeography and population structure of the red stingray, *Dasyatis akajei* inferred by mitochondrial control region. Mitochondr DNA 26(4): 505–513

McManus JFA (1946) Histological demonstration of mucin after periodic acid. Nature 158(4006): 202–202

Pärt P, Wright PA, Wood CM (1998) Urea and water permeability in dogfish (*Squalus acanthias*) gills. Comp Biochem Physiol A 119(1): 117–123

Payan P, Goldstein L, Forster RP (1973) Gills and kidneys in ureosmotic regulation in euryhaline skates. Am J Physiol 224(2): 367–372

Piermarini PM, Evans DH (1998) Osmoregulation of the Atlantic stingray (*Dasyatis sabina*) from the freshwater Lake Jesup of the St. Johns River, Florida. Physiol Zool 71(5): 553–560

Rahmatullah M, Boyde TRC (1980) Improvements in the determination of urea using diacetyl monoxime; methods with and without deproteinisation. Clin Chim Acta 107(1–2): 3–9

Smith HW (1929) The composition of the body fluids of elasmobranchs. J Biol Chem 81(2): 407–419

Smith HW (1936) The retention and physiological role of urea in Elasmobranchii. Biol Rev 11: 49–82

Stolte H, Galaske RG, Eisenbach GM, Lechene C, Schmidt-Nielsen B, Boylan JW (1977) Renal tubule ion transport and collecting duct function in the elasmobranch little skate, *Raja erinacea*. J Exp Zool 199(3): 403–410

Takabe S, Teranishi K, Takaki S, Kusakabe M, Hirose S, Kaneko T, et al. (2012) Morphological and functional characterization of a novel Na^+/K^+-ATPase-immunoreactive, follicle-like structure on the gill septum of Japanese banded houndshark, Triakis scyllium. Cell Tissue Res 348(1): 141–153

Takagi W, Kajimura M, Bell JD, Toop T, Donald JA, Hyodo S (2012) Hepatic and extrahepatic distribution of ornithine urea cycle enzymes in holocephalan elephant fish (*Callorhinchus milii*). Comp Biochem Physiol B 161: 331–340

Thurau K, Antkowiak D, Boylan JW (1969) Demonstration of a renal osmoregulatory mechanism in the spiny dogfish, Squalus acanthias. Bull Mr Desert Island Biol Lab 9: 63–64

Wong TM, Chan DKO (1977) Physiological adjustments to dilution of the external medium in the lip-shark *Hemiscyllium plagiosum* (Bennett). II. Branchial, renal and rectal gland function. J Exp Zool 200(1): 85–95

Yamaguchi Y, Takaki S, Hyodo S (2009) Subcellular distribution of urea transporter in the collecting tubule of shark kidney is dependent on environmental salinity. J Exp Zool 311: 705–718